Astronomy & Astrophysics manuscript no. crab˙paper
February 26, 2017

Polarization Spectral Energy Distribution of the Crab Nebula in prospect of future CMB experiments

Address(es) of author(s) should be given

Received February 26, 2017 / Accepted –

Abstract

The detection of the primordial B-modes constitutes one of the major challenges of modern cosmology. The precise measurement of this signal requires an accurate determination of foreground contaminants and the absolute calibration of the instrument in terms of cross polarization and absolute polarization angle reconstruction. We present here a study of the well known polarization angle calibration source: the Crab nebula. It represents the most intense source in the microwave sky with an extension of few arcminutes corresponding to the typical beam of CMB experiments. The Crab nebula exhibits a highly polarized synchrotron radiation at radio and millimeter wavelengths. In this paper we present Crab Stokes I, Q and U maps obtained at 150 GHz with the *NIKA* camera. *NIKA* has been operated at IRAM 30 m telescope from 2012 to 2015. It is a camera made of Lumped Element Kinetic Inductance Detectors (LEKIDs) and observing the sky at 150 and 260 GHz. Taking advantage from previous observations of the Crab Nebula in intensity and polarization, we report in this paper the polarization spectral energy distribution (SED).

Key words. Techniques: polarization – KIDs – individual: NIKA

1. Introduction

The polarization of the Cosmic Microwave Background (CMB) anisotropies offers a powerful way to investigate the early Universe. They can be decomposed into a scalar and a pseudo-scalar field, respectively called E and B modes. The primordial density fluctuations (scalar perturbations) can only produce E CMB polarization, while B CMB polarization can only be produced by primordial (tensor perturbations) gravitational waves (Polnarev 1985; Seljak & Zaldarriaga 1997) arising from the inflationary epoch (Guth 1981; Linde 1982) and by gravitational lensing of the $E-$modes (Ade et al. 2015). The detection of the primordial $B-$modes could definitively probe the existence of an inflationary epoch and constitutes one of the most ambitious goals of the modern observational cosmology.

Recently, BICEP2/Keck and Planck Collaborations et al. (2015); BICEP2 Collaboration et al. (2016) set a 95% upper limit for the detection of the tensor to scalar ratio $r < 0.07$. Upcoming CMB experiments aiming at measuring the primordial $B-$modes require an accurate determination of the foreground emissions to the CMB signal and a high control of the systematic effects. One of the most difficult parameters to be characterized for a CMB polarization experiment is the calibration of residual cross polarization and of the absolute polarization angle. This can be achieved using observations of well known polarized sources like the Crab nebula.

The Crab Nebula (or Tau A) located at equatorial coordinates $\alpha = 5^h34^m32s$ and $\beta = 22°0'52''$ is a plerion-type supernova remnant emitting a highly polarized signal. A synchrotron emission from the nebula is observed in the radio frequency domain, which is powered by a pulsar through its jet. Moreover, near the center of the nebula we observe a shock, which is formed where the jet is thermalized and ultra-relativistic particles are released into the surrounding nebula. This source represents the most intense polarized astrophysical object in the microwave sky at angular scales of few arcminutes and for this reason it is of particularly interest for the calibration of a CMB polarization experiment, which has a typically beam comparable to the extension of the source. For a detailed review on this source we refer to Hester (2008).

The Crab nebula has been already used for polarization cross-check analysis in the frequency range from 30 to 353 GHz of the *Planck* satellite mission. High angular resolution observations achieved by the XPOL experiment (Thum et al. 2008) from the IRAM 30 m telescope have shown the spatial distribution of the Crab Nebula in intensity and polarization at 90 GHz with an absolute accuracy of 0.5° in the polarization angle (Aumont et al. 2010). High angular resolution observations of the Crab nebula in polarization could be very useful for the calibration of the next generation of polarization experiments. In particular those aiming at a precise measurement of the CMB polarization, which have a large frequency range to be able to carefully study the foreground emissions.

Previous studies (Macías-Pérez et al. 2010) of the total flux density of the Crab nebula have shown a spectrum well described by a single synchrotron component, and predict negligible variations in polarization fraction and angle in the frequency of interest for CMB studies.

Polarized observations of the Crab Nebula have been performed with the *NIKA* camera from the IRAM 30 m telescope during the observational campaign of February, 2015. A first report on this source has been discussed in (Ritacco et al. 2016). In order to trace the polarized Spectral Energy Density (SED) we used polarization observations performed by the WMAP satellite at 23, 33, 41, 61 and 94 GHz (Weiland et al. 2011), *Planck* satellite at 30, 44, 70, 100, 143, 217, 353 GHz and XPOL at 90 GHz (Aumont et al. 2010). The paper is organized as follows: in Sec. 2 the intensity and polarization maps performed with the *NIKA* camera are presented together with the polarization degree and angle spatial distribution; Sec. 3 presents the reconstruction of the polarization properties in well defined regions to for comparison with CMB like beams experiments; Sec. 4 presents the Crab nebula SED; Sec. 5 we draw the conclusions.

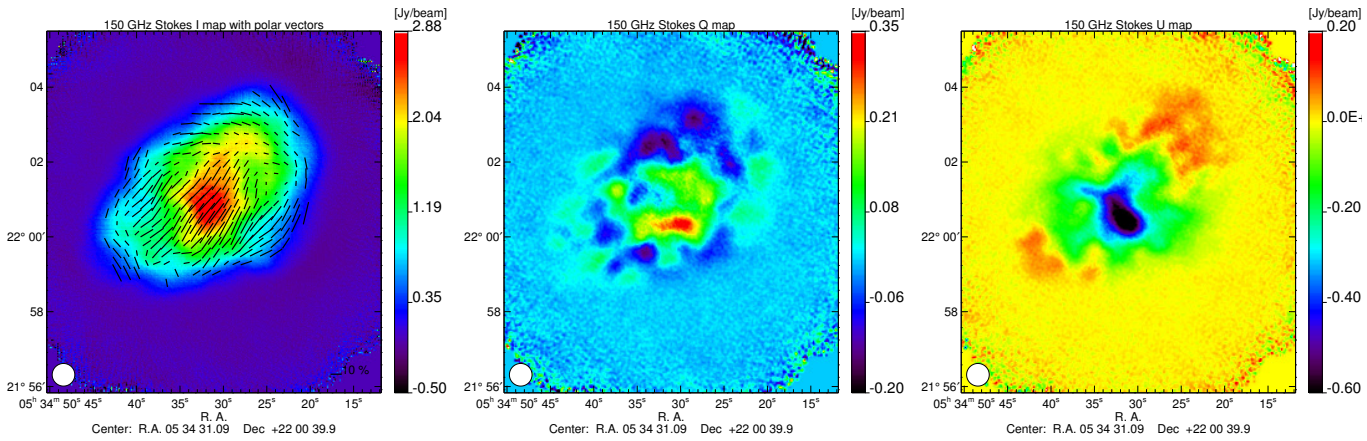

Figure 1. From left to right: Crab nebula Stokes I, Q and, U maps obtained at 150 GHz with the *NIKA* camera. Polarization vectors, indicating both the degree and the orientation, are over-plotted in black on the intensity map where the polarization intensity P > 3 σ_P.

2. *NIKA* observations of the Crab Nebula

2.1. NIKA camera

NIKA is a dual band camera observing the sky at 150 and 260 GHz with 18″ and 12″ FWHM resolution, respectively. It has been operated at the IRAM 30 telescope between 2012-2015. A detailed description of the *NIKA* camera can be found in Monfardini et al. (2010, 2011); Catalano et al. (2014). In addition to the measurements in intensity it was also a test bench for polarization facilities of the final instrument *NIKA2*, installed at the telescope on October, 2015 (Calvo et al. 2016; Catalano et al. 2016). A previous paper (Ritacco, A. et al. 2017) gives more details on *NIKA* polarization facilities and it describes the performances of the instrument at the telescope. The characterization of the *NIKA* polarization capabilities has been very important to get prepared for the follow-up camera *NIKA2*. Beyond that, *NIKA* provided the first polarization observations performed with KIDs. Unfortunately, the observations of the Crab nebula performed at 260 GHz have been limited by the sensitivity of the *NIKA* instrument in polarization and the resulting maps show a no significant detection, for that reason here we discuss only the observations performed at 150 GHz.

2.2. NIKA observations

In order to obtain polarization maps a dedicated data analysis pipeline has been developed and described in Ritacco, A. et al. (2017). The Stokes I, Q and, U maps shown in Fig. 1 have been obtained by a combination of 16 observational scans of 8 × 6 arcminutes for a total observation time of ∼ 2.7 hours performed during the observational campaign of February 2015. In order to have the best coverage of the source surface we performed on-the-fly maps oriented in equatorial coordinates according to four different scan directions: 0°, 90°, 120°, 150°. For an extended source like the Crab nebula, with angular size bigger than *NIKA* beams, it is difficult to properly estimate its intensity emission avoiding filtering effects due to noise decorrelation methods. The "classical" common mode decorrelation method used consists on the use of only the pixels outside the source to reconstruct the template to be subtracted. Filtering effects can be encountered in regions where the number of pixels used for the decorrelation is too low. This occurs observing sources more extended than the beam of the instrument, like the Crab nebula. In order to avoid such an effect the Stokes I map shown on the left panel of Fig. 1 has been obtained by using a decorrelation method called "dual-band decorrelation". Such a decorrelation algorithm has been developed for the reconstruction of the Sunyaev-Zel'dovich signal in galaxy clusters observations (Adam et al. 2014) taking advantage of *NIKA* dual-band capabilities. The idea of this algorithm arises with the fact that the atmospheric emission is stronger at 260 GHz than at 150 GHz, as a consequence we can use 260 GHz observations as a "template" to be subtracted to the 150 GHz observational data.

Further, we identified an intensity to polarization leakage effect observing Uranus, which is expected to be unpolarized. In order to correct for this effect an algorithm has been developed and applied to all the *NIKA* observations performed in polarization. This effect together with the leakage correction algorithm is well described in Ritacco, A. et al. (2017).

The observed signal reaches a value of 0.5% peak-to-peak of the total intensity. The level of this spurious instrumental polarization is significantly lower than the observed one on Uranus. This is probably due to a compensation of the negative and positive signal between adjacent pixels. Although the leakage effect is very weak on this diffuse source the correction is still applied to produce the final maps presented in Fig. 1.

2.3. Crab polarization properties

In this section we discuss the polarization properties of the source in terms of polarization degree p and angle ψ, which are defined through the Stokes parameters I, Q, and U as follows:

$$p = \frac{\sqrt{Q^2 + U^2}}{I}$$
$$\psi = \frac{1}{2} \arctan \frac{U}{Q}. \quad (1)$$

These definitions are not linear in I, Q and U and are biased by the noise. Where the signal-to-noise ratio is too low (*i.e.* $Q \simeq U \simeq 0$) the noise measured on Q and U maps will yield a non-zero degree of the polarization estimate. Simmons et al. (1980); Simmons & Stewart (1985); Montier et al. (2015) proposed analytical solutions to correct this bias. However, at the

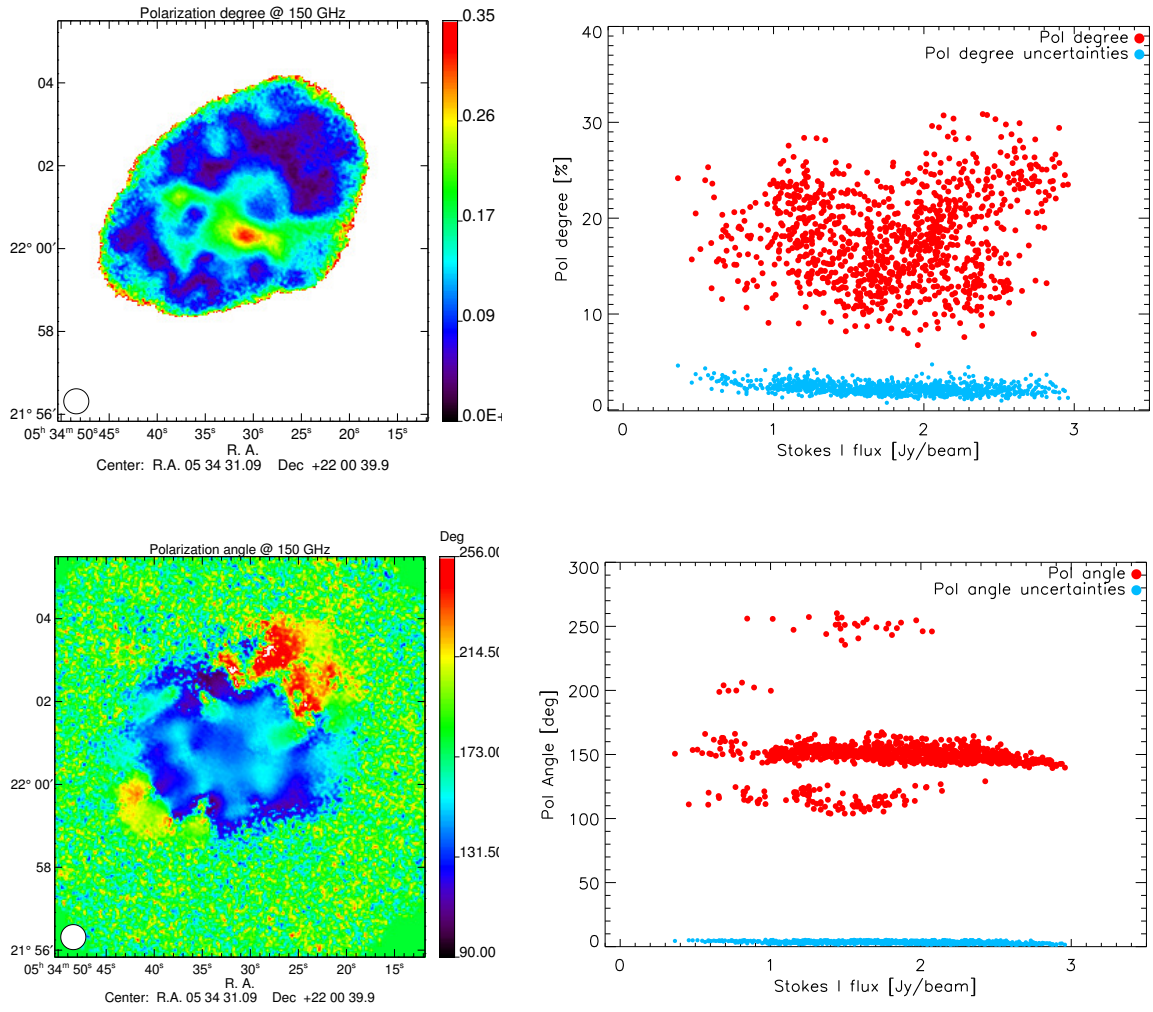

Figure 2. *Top*: polarization degree naive estimator map p (left) of the Crab nebula. Noise bias corrected values of p are represented on the right panel as a function of the Stokes I total intensity map where the polarization intensity $P > 5\sigma_P$. *Bottom*: polarization angle map ψ (left) of the Crab nebula. Polarization angle ψ where $P > 5\sigma_P$ vs the Stokes I total intensity map. The cyan dots represent the uncertainties calculated as the dispersion between different scans.

limit of high S/N ratio which the estimation of the polarization degree and its uncertainty become:

$$p = \frac{\sqrt{Q^2 + U^2 - \sigma_Q^2 - \sigma_U^2}}{I},$$
$$\sigma_p = \frac{\sqrt{Q^2\sigma_Q^2 + U^2\sigma_U^2 + p^4 I^2 \sigma_I^2}}{pI^2}. \quad (2)$$

Furthermore, the polarization angle in a high S/N regime can be approximated by the classical Eq. 1 with uncertainty

$$\sigma_\psi = \frac{\sqrt{Q^2\sigma_Q^2 + U^2\sigma_u^2}}{2(pI)^2}. \quad (3)$$

For the representation of the polarization degree and angle maps (left panels of Fig. 2) we keep the standard representation (see Eq. 1) to ease the comparison with other experiments, which usually adopt this convention. This choice is however a valid approximation because of the high signal to noise ratio observed on the maps. By contrast, the right panels show the debiased (see Eq. 2) values of polarization degree and angle as function of the Stokes intensity I map, where the polarization intensity P= $\sqrt{Q^2 + U^2} > 5\,\sigma_P$. The distribution of the polarization degree in Fig. 2 appears highly dispersed around a polarization degree value of ∼ 20-30±4%.

The spatial distribution of ψ presented on the bottom right panel of the figure shows a value of the angle ≃ 150° represented here in equatorial coordinates, which remains approximately constant in the central region of the source. On the map edges, ψ pixel-to-pixel deviation is high, except for the northern region where the average angle is around 220°. This particular effect has been already observed by the XPOL experiment at 90 GHz (Aumont et al. 2010). This together with the variation of the polarization fraction and angle observed confirms the need of high angular resolution observations at low and high frequencies for a good understanding of the source polarized emission.

The polarization intensity P is also represented in Fig. 3. We can clearly identify the high polarization emission located near the pulsar position and the surrounding gas.

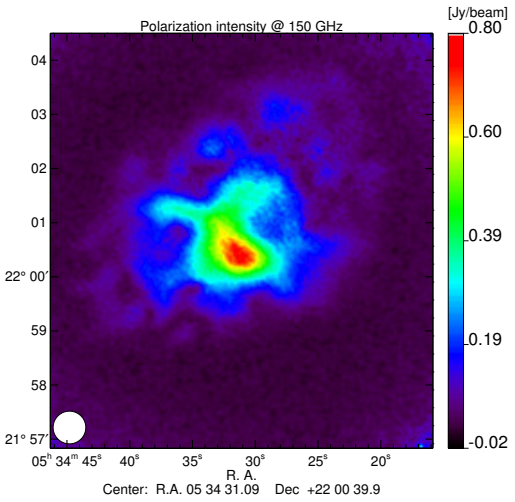

Figure 3. Polarization intensity map obtained at 150 GHz. The map shows the high polarized emission of this source reaching a value of 0.8 Jy beam^{-1}.

3. Total intensity and polarization in well defined regions

The angular extension of the Crab nebula is 4′. In order to have an estimation of the flux in this region we calculate the integrated flux as shown in Fig. 4. A zero level, calculated as the mean of the signal measured on an external annular ring region, has been subtracted from the flux. The maximum signal estimated in this region is 204.4±7.9±10.2 Jy. The first uncertainty accounts for statistical uncertainties computed from fluctuations of the signal at large radii. The second term of the uncertainty indicates the calibration error corresponding to ≃ 5% at 150 GHz. This absolute error is estimated as the dispersion of all the Uranus observations collected during the observational campaign.

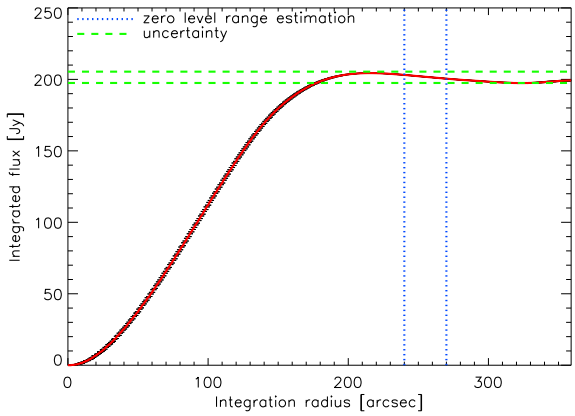

Figure 4. Integrated flux estimated up to 4′. The flux has been corrected by a zero level, which corresponds to the mean of the signal calculated in an annular ring indicated by the blue dotted lines. The green dotted line represents the uncertainties measured at large radii.

3.1. Polarization estimates in CMB experiments like beams

In order to compare with low angular resolution CMB experiments we give here the polarization degree p and angle ψ integrated values obtained in well defined regions. Tab. 1 shows the total intensity I, polarized intensity P, polarization degree p and polarization angle ψ obtained in four different regions. In order to compare with *Planck* satellite we estimate the values in two regions of 7′ and 5′ corresponding to the beams of the *Planck* frequency channels at 143 and 217 GHz, respectively. Further, two regions are defined with high S/N ratio. First, where $P > 3\sigma$ and then, referring to the polarization intensity P (see Fig. 3) around the peak of the signal where $P > 0.2$ Jy. In Tab. 1 the polarization angles are represented in Galactic coordinates to ease the comparison with *Planck* (Planck Collaboration et al. 2015) and *WMAP* CMB experiments (Weiland et al. 2011). The difference between the polarization angles found can be explained by the fact that we account for low S/N regions in the estimation of the Stokes I, Q and, U fluxes. For the comparison with other instruments we choose the polarization angle estimated in 5′ and where $P > 3\sigma$ as best estimator. This latter is represented in red in Fig. 5, the uncertainty accounts for statistical estimation and the systematic uncertainty of 1.8°. It is furthermore in a very good agreement with the result found by *Planck* at 143 GHz and it is in agreement at 1σ with all the observations.

Fig. 5 shows the polarization fraction (top) and angle (bottom) as function of the frequency for five different instruments: *Planck*, WMAP, XPOL, SCUPOL and *NIKA*. Notice that SCUPOL maps (Matthews et al. 2009) provided at 352 GHz have reduced angular size w.r.t *NIKA*. For that reason we define a small region of 1.4′ around the peak of the polarization intensity. For the polarization fraction we keep the convention used by XPOL (Aumont et al. 2010) and we represent in the figure the value measured in 5′. The solid line in both figures represents the mean value found using all the observations shown and the uncertainty represents the standard deviation.

NIKA and XPOL polarization fraction estimates are not consistent. This can be explained by the difference observed in the estimation of total intensity for both instruments. A lower total intensity measured produces a higher polarization degree. Notice that by referring to Fig. 6 the value obtained by *NIKA* at 150 GHz appears well consistent with previous experiments, whereas XPOL intensity is a bit low with respect to what expected by power law estimated by (Macías-Pérez et al. 2010) and the best-fit model estimated in this paper.

4. Crab SED

4.1. Intensity

As previously stated observing the Crab nebula is particularly interesting for its angular extension, which is compatible with the typical beam of a CMB experiment, and for its stability across the millimeter wavelengths range. Its total intensity emission at millimeter wavelengths (1 and 10^6 GHz) is well described by a synchrotron spectrum decreasing with the frequency, which has the form:

$$I_\nu = A(\nu/1GHz)^\beta \quad (4)$$

with spectral index β = -0.296±0.06 (Baars et al. 1977; Macías-Pérez et al. 2010). At submillimeter wavelengths (10-100 μm) a cold dust component is also observed. Further, the Crab nebula is fading with time at a rate of α = 0.167±0.015 % yr^{-1} (Aller & Reynolds 1985). These observations suggest a low frequency

	I [Jy]	P [Jy]	p [%]	ψ [°]
P > 3 σ_P	84.6±0.01	10.51 ±0.01	12.42±0.01	-87.15 ±0.04±1.8(syst)
seen by 1.4′ with P > 0.2 Jy	60.6±0.2	10.28±0.01	16.96±0.01	-87.69±0.01±1.8(syst)
seen by 5′	219.0±0.1	14.8 ±0.03	6.78±0.01	-83.7±0.1±1.8(syst)
seen by 7′	231.8±0.2	14.03±0.09	6.05±0.04	-85.1±0.5±1.8(syst)

Table 1. Total intensity I flux and polarized intensity flux P, polarization degree p, and angle ψ. The values have been calculated in the region with high S/N and within 5′ and 7′ from the center of the source. A calibration error of 5 % has to be accounted for and propagated to the polarization estimates. The systematic uncertainty of 1.8° is due to the HWP zero position.

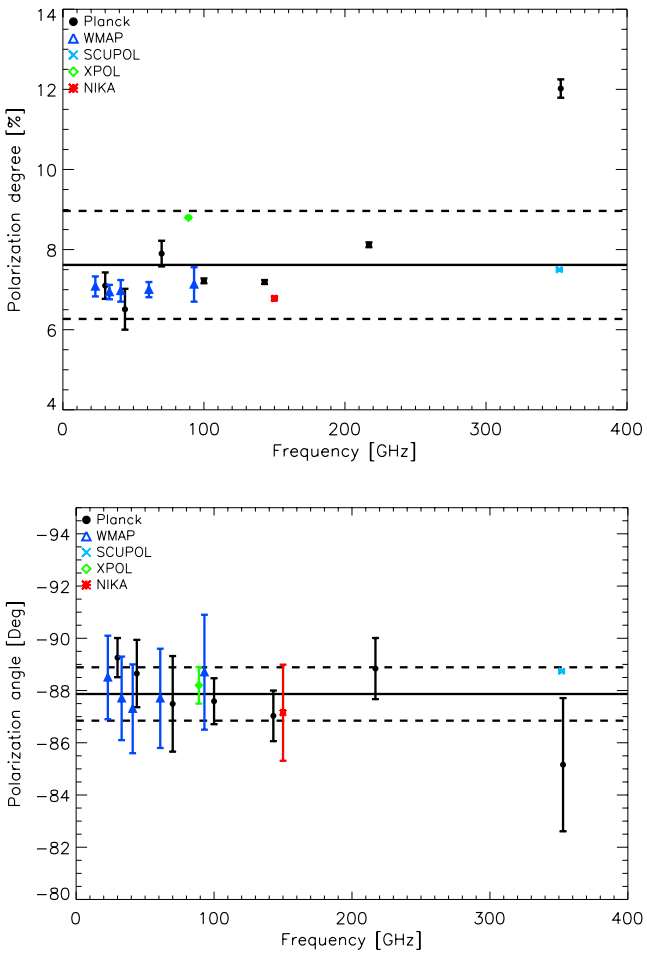

Figure 5. *Top*: polarization degree as a function of frequency as measured by *Planck*, WMAP, XPOL, SCUPOL and *NIKA* (red). *NIKA* value has been estimated by integrating in a radius of 5′ as given by XPOL (Aumont et al. 2010). The SCUPOL estimated in 1.4′ around the peak of the polarization intensity from the maps in the SCUBA catalogue (Matthews et al. 2009). *Bottom*: polarization angles in Galactic coordinates for the four experiments given above.

emission produced by particles accelerated by the same magnetic field. The direction of the polarization is thus expected to be constant while the polarization degree may vary.

In order to compare the *NIKA* results with previous analysis we represent in Fig. 6 the intensity flux of the Crab nebula as a function of the frequency. The "radio experiments" in the plot refer to values reported in (Dmitrenko et al. 1970; Vinogradova et al. 1971). We also include *Archeops* (Macías-Pérez et al. 2007), *Planck* (Planck Collaboration et al. 2015), WMAP (Weiland et al. 2011) and MAMBO (Bandiera et al. 2002). *NIKA* intensity flux obtained at 150 GHz is shown in red. The fit model obtained by a previous analysis (Macías-Pérez et al. 2010) is shown in green. The coefficients of best-fit model (cyan) is obtained by χ^2 minimization for observations at ν <100 GHz are:

$$A = 980.6 \pm 0.7, \quad \beta = -0.3151 \pm 0.0002. \tag{5}$$

Notice that fading is accounted for in the best-fit estimation as well as in the data represented in figure, to ease the interpretation of the plot. The *Planck* measurements obtained at 100, 143, 217 and 353 GHz suggest an another power law component in the Crab, unexpected at these frequencies, maybe due to the contribution of another population of electrons, which produce a sweeping change in the spectrum at the knee frequency of 90 GHz. The coefficients of the fit in the frequency range 100 < ν < 360 GHz are: A = 8.6 ± 0.45 and β = -0.71 ± 0.09. By contrast high angular resolution results provided by *NIKA* and MAMBO at 230 GHz are in contrast with this behaviour at higher frequency than 100 GHz. Further high angular resolution observations in this frequency range could provide a better understanding of the emission spectrum.

The estimated best-fit model (cyan line) is a bit different w.r.t the previous analysis provided by (Macías-Pérez et al. 2010) mainly because of the addition of recently published results by *Planck* (Planck Collaboration et al. 2015) and WMAP (Weiland et al. 2011). However, the result found at 150 GHz by the *NIKA* camera agrees in 1 σ uncertainty both models. It is also in agreement within 2 σ with the estimated fit at higher frequencies found using *Planck* observations.

4.2. Polarization

The total intensity of the Crab nebula has been monitored along decades across a large range of frequency but the polarization amount of observations is really poor. The recent results provided by *Planck* (Planck Collaboration et al. 2015), *WMAP* (Weiland et al. 2011), XPOL (Aumont et al. 2010) allow together with *NIKA* to trace the polarization intensity SED, see Fig. 7. The different values measured by *Planck* are quite different between each other, while the *WMAP* results are consistent with a power law decreasing with the frequency. Assuming a power law as described by the Eq. 4.1 we estimate two models represented in blue and black on the figure account for only *WMAP* data and *Planck* data, respectively. Accounting for fading the fitted amplitude and spectral indexes β are:

– fit results using only the WMAP data:

$$A = 78.9 \pm 7.8 \quad , \quad \beta_p = -0.35 \pm 0.03; \tag{6}$$

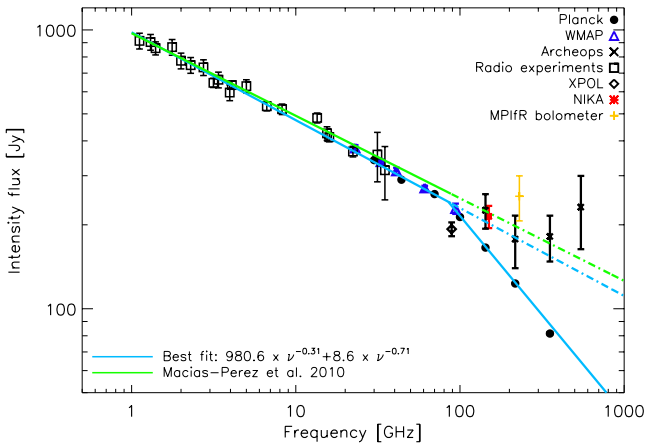

Figure 6. Crab nebula total intensity SED. The green line shows the model derived by a previous analysis discussed in (Macías-Pérez et al. 2010). The best-fit obtained by a new analysis is shown in cyan line. Both, the fit and the data account for the fading with the time.

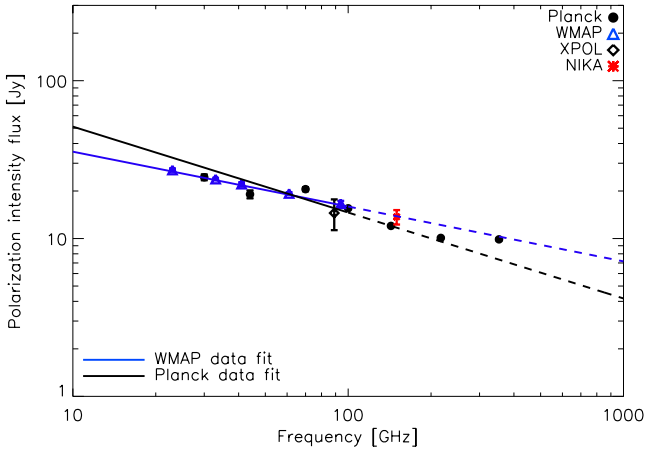

Figure 7. Crab nebula polarization intensity SED. The two best-fit models presented have been estimated using only WMAP data (blu line) or *Planck* data only (black line).

– fit results using only the *Planck* data:

$$A = 179.1 \pm 15.4 \quad , \quad \beta_p = -0.54 \pm 0.02. \qquad (7)$$

The "*WMAP*" fit is generally consistent with itself and with *Planck* observations at 30, 100 and 353 GHz. *NIKA* result obtained at 150 GHz is well consistent with this model and also consistent in 1σ with the "*Planck*' fit. By contrast, the *Planck* data have a significantly steeper spectral index. This model is not consistent neither with the *Planck* observation at 70 and 353 GHz nor with the *WMAP* observations except for the point at 61 GHz.

As already discussed above, the controversial interpretation of these two models confirm the need of new mm wavelengths polarization observations. Moreover, we take advantage from previous observations performed by SCUPOL at 352 GHz (850 μm) to estimate the spectral index β_p = -0.33 ± 0.01. This latter is in a very good agreement with the estimation of the spectral index using the SED and the model derived using WMAP observations.

5. Conclusions

This paper presents the Crab nebula polarization observations performed at 150 GHz by the *NIKA* camera. Such high angular resolution observations allows to trace the spatial distribution of the polarization fraction and angle. We also estimate the polarization proprieties in well defined regions on the source, allowing the comparison with CMB experiments, which have a typical beam of 5′. The value that we assume as best estimator of the polarization angle is -87.15±0.04±1.8. We found generally a consistency with *Planck*, *WMAP* and XPOL previous observations. The polarization degree is also consistent and vary depending on the region considered as expected. We present here also the first estimation of the Crab polarization intensity SED. Taking advantage from previous observations of *WMAP* and assuming a synchrotron like power law we estimate the best-fit model with coefficients: A = 78.9±7.8 β_p = -0.35±0.03. *NIKA* polarization intensity result is a very good agreement with this model. The estimation of the spectral index using SCUPOL observation at 352 GHz and *NIKA* at 150 GHz gives β_p = -0.33±0.01, confirming the result found previously on the SED. From the analysis presented here we clearly need more polarization high angular resolution observations in the frequency range from 100 to 500 GHz to better understand the discrepancy found between, for example, *Planck* results in total intensity and polarization with other observations.

Acknowledgements. We would like to thank the IRAM staff for their support during the campaigns. The NIKA dilution cryostat has been designed and built at the Institut Néel. In particular, we acknowledge the crucial contribution of the Cryogenics Group, and in particular Gregory Garde, Henri Rodenas, Jean Paul Leggeri, Philippe Camus. This work has been partially funded by the Foundation Nanoscience Grenoble, the LabEx FOCUS ANR-11-LABX-0013 and the ANR under the contracts "MKIDS", "NIKA" and ANR-15-CE31-0017. This work has benefited from the support of the European Research Council Advanced Grant ORISTARS under the European Union's Seventh Framework Programme (Grant Agreement no. 291294). We acknowledge fundings from the ENIGMASS French LabEx (R. A. and F. R.), the CNES post-doctoral fellowship program (R. A.), the CNES doctoral fellowship program (A. R.) and the FOCUS French LabEx doctoral fellowship program (A. R.).

References

Adam, R., Comis, B., Macías-Pérez, J. F., et al. 2014, A&A, 569, A66
Ade, P., Aghanim, N., Ashdown, M., et al. 2015, arXiv preprint arXiv:1512.02882
Aller, H. & Reynolds, S. 1985, The Astrophysical Journal, 293, L73
Aumont, J., Conversi, L., Thum, C., et al. 2010, A&A, 514, A70
Baars, J., Genzel, R., Pauliny-Toth, I., & Witzel, A. 1977, Astronomy and Astrophysics, 61, 99
Bandiera, R., Neri, R., & Cesaroni, R. 2002, A&A, 386, 1044
BICEP2 Collaboration, Keck Array Collaboration, Ade, P. A. R., et al. 2016, Physical Review Letters, 116, 031302
BICEP2/Keck and Planck Collaborations, Ade, P. A. R., Aghanim, N., et al. 2015, ArXiv e-prints
Calvo, M., Benoit, A., Catalano, A., et al. 2016, ArXiv e-prints
Catalano, A., Adam, R., Ade, P., et al. 2016, ArXiv e-prints
Catalano, A., Calvo, M., Ponthieu, N., et al. 2014, A&A, 569, A9
Dmitrenko, D., Tseitlin, N., Vinogradova, L., & Giterman, K. F. 1970, Radiophysics and Quantum Electronics, 13, 649
Guth, A. H. 1981, Phys. Rev. D, 23, 347
Hester, J. J. 2008, ARA&A, 46, 127
Linde, A. D. 1982, Physics Letters B, 108, 389
Macías-Pérez, J., Lagache, G., Maffei, B., et al. 2007, Astronomy & Astrophysics, 467, 1313
Macías-Pérez, J. F., Mayet, F., Aumont, J., & Désert, F.-X. 2010, ApJ, 711, 417

Matthews, B. C., McPhee, C. A., Fissel, L. M., & Curran, R. L. 2009, ApJS, 182, 143
Monfardini, A., Benoit, A., Bideaud, A., et al. 2011, ApJS, 194, 24
Monfardini, A., Swenson, L. J., Bideaud, A., et al. 2010, A&A, 521, A29
Montier, L., Plaszczynski, S., Levrier, F., et al. 2015, A&A, 574, A136
Planck Collaboration, Ade, P. A. R., Aghanim, N., et al. 2015, ArXiv e-prints
Polnarev, A. 1985, Soviet Astronomy, 29, 607
Ritacco, A., Adam, R., Adane, A., et al. 2016, Journal of Low Temperature Physics, 184, 724
Ritacco, A., Ponthieu, N., Catalano, A., et al. 2017, A&A, 599, A34
Seljak, U. & Zaldarriaga, M. 1997, Physical Review Letters, 78, 2054
Simmons, J. F. L., Aspin, C., & Brown, J. C. 1980, A&A, 91, 97
Simmons, J. F. L. & Stewart, B. G. 1985, A&A, 142, 100
Thum, C., Wiesemeyer, H., Paubert, G., Navarro, S., & Morris, D. 2008, PASP, 120, 777
Vinogradova, L. V., Dmitrenko, D. A., & Tsejtlin, N. M. 1971, Izvestiia Vysshaia Uchebn. Zaved., Radiofizika, 14, 157
Weiland, J. L., Odegard, N., Hill, R. S., et al. 2011, ApJS, 192, 19